Anthropologica et Præhistorica, 126/2015 (2016) : 91-104

Mineralogy, Geochemistry and Microstructure of Post-Tertiary Kaolinitic Hematite from Rajasthan State, NW India

Giovanni CAVALLO & Manoj K. PANDIT

Résumé

Les échantillons d'hématite kaolinitique ont été récoltés au centre sud de la région des montagnes de Aravalli (AMR), dans le district de Chittourgarh, Rajasthan, Inde. Des analyses de la microstructure, de la composition chimique et minéralogique ont été effectuées à l'aide de MLP, MEB/EDS, DRX, FRX.

L'utilisation de techniques basées sur l'emploi du microscope et des techniques micro analytiques ont permis de faire la distinction entre une structure massive où des reliques de minéraux semblables aux plagioclases sont préservés et des microstructures semblables à des ooïdes (glaebules). Ces dernières ont été regroupées en quatre typologies en fonction de la distribution et de la concentration relative de Si, Al et Fe. En particulier, les microstructures sphériques montrent des noyaux riches en Fe entourés par une bordure fine, riche en Al (Type A), des noyaux riches en Al entourés par une bordure fine riche en Fe (Type B), Al associé à des noyaux riches en Al-Si avec une bordure en Al-Si (Type C) et des particules subarrondies riches en Al où l'Al est associé à des grains d'oxydes et à du Si (Type D). Le diamètre est compris entre 70 et 250 µm.

Tous les échantillons contiennent de la kaolinite [$Al_2Si_2O_5(OH)_4$], de l'hématite (α-Fe_2O_3) et de l'anatase (TiO_2). Sur la base du rapport ordre-désordre de la structure de la kaolinite il a été possible de rassembler les échantillons en un Type I, avec de la kaolinite ordonnée, et en un Type II où le désordre peut être mis en évidence grâce aux pics caractéristiques des diffractogrammes aux rayons X. Les pics de l'hématite et de l'anatase sont larges ce qui indique une cristallinité basse.

La majorité des échantillons ont des pertes au feu >10 %, ce qui souligne leur état très altéré. Des contenus presque négligeables en alcalis confirment cette interprétation étant donné leur mobilité élevée dans tous les processus qui se déroulent dans la croûte terrestre. Les teneurs en TiO_2 sont anormalement élevées et sont, en général, positivement corrélées avec les valeurs de Al_2O_3. Al et Ti sont tous les deux très résistants et peu mobiles pendant les processus d'hydratation et d'altération. Un rapport inversement proportionnel entre SiO_2 et TiO_2 confirme cette interprétation. Le SiO_2 est corrélé positivement avec la perte au feu ce qui confirme ultérieurement que le SiO_2 est le principal composant qui a été lessivé pendant le processus d'altération. Des valeurs élevées et variables de Fe_2O_3 indiquent soit que les roches étaient riches en Fe soit qu'il y a eu un enrichissement durant le processus d'altération. L'absence de corrélation systématique entre TiO_2 et Fe_2O_3 suggère qu'il y a eu un enrichissement secondaire en fer durant le processus d'altération. La composition chimique totale (valeurs basses pour SiO_2 et élevées pour Al_2O_3, TiO_2, Fe_2O_3) indiquent que les roches à l'origine de ces argiles hématitiques étaient de nature basique (probablement des basaltes). Leur source potentielle pourrait être la large étendue des basaltes du Deccan (Crétacé final à base du Tertiaire) qui couvrent la région de Chittourgarh. Quelques échantillons très riches en silicium peuvent être attribués à des shales et à des grès protérozoïques appartenant au Super groupe Vindhyan qui sont sous les basaltes L'altération des roches hôtes en hématite kaolinique est donc un évènement post-Tertiaire.

Ce travail représente un premier essai de caractérisation de l'hématite kaolinitique dans le but de disposer d'une banque de données ce qui est essentiel pour des études de provenance d'hématites utilisées dans d'objets archéologiques et historiques en hématite.

***Mot-clés** : ocre rouge, microstructure de l'ocre, géochimie de l'ocre, kaolinite, hématite, anatase, Rajasthan, Inde du Nord-Ouest.*

Abstract

Mineralogical, geochemical and microstructural characteristics of kaolinitic hematite samples from Chittourgarh in the south-central part of the Aravalli Mountain Region (AMR) in Rajasthan State, NW India, are presented and discussed. The analytical techniques used were PLM, SEM/EDS, XRD, XRF.

Microscopic observations and microanalysis allowed to differentiate a massive microstructure where relics of plagioclase-like minerals are still preserved and ooid-like microstructures (glaebules) can be seen. Glaebules were grouped into four types according to relative concentrations of Si, Al, and Fe and their distribution. The rounded microstructures exhibit Fe-rich cores surrounded by a thin Al-rich rim (Type A), Al-rich cores surrounded by a thin Fe-rich rim (Type B), Al associated with Al-Si rich cores by a Al-Si rim (Type C) and Al-rich sub-rounded particles where Al is both related to oxide grains and to Si (Type D). The diameter ranges between 70 to 250 μm.

All the samples contain kaolinite [$Al_2Si_2O_5(OH)_4$], hematite (α-Fe_2O_3) and anatase (TiO_2). Based on the order-disorder in kaolinite structure it was possible to group the samples in Type I where ordered kaolinite was detected and Type II where disorder is clearly displayed by characteristic XRD reflections. Hematite and anatase reflections are rather broad indicating poor-crystalline mineral phases.

The majority of the samples have >10 % LOI (loss on ignition), underlining their heavily altered nature. Almost negligible alkali contents further substantiate this interpretation as these are highly mobile in any crustal process. TiO_2 values are unusually high and also generally correlate positively with Al_2O_3. Both Al and Ti are extremely resistant and immobile during hydration and alteration processes. An inverse relationship between SiO_2 and TiO_2 also attests to this proposition. The SiO_2 correlated positively with LOI, further confirming that the SiO_2 was the major component that was lost during alteration. High and variable Fe_2O_3 values show both an iron rich rock as well as iron enrichment during alteration process. Lack of any systematic correlation between TiO_2 and Fe_2O_3 suggests secondary iron enrichment during alteration. Overall geochemistry (low SiO_2, high Al_2O_3, TiO_2 and Fe_2O_3) indicate basic rocks (most likely, basalt) as the provenance for these iron rich clays. The potential source could be the vast expanse of Late Cretaceous – Early Tertiary Deccan basalts that are exposed in the Chittourgarh region. Some high silica samples may be attributed to shale and sandstones belonging the Proterozoic Vindhyan Supergroup that underlie the basalts. The alteration of host rocks into secondary kaolinitic hematite is therefore a post Tertiary event.

This study is the first attempt to characterize kaolinitic hematite in order to develop a preliminary database essential for provenance studies of hematite used in archaeological and historical artefacts.

Keywords: red ochre, ochre microstructure, ochre geochemistry, kaolinite, hematite, anatase, Rajasthan, NW India.

1. INTRODUCTION

In the economic geological context the term "ochre" is loosely used to designate clay minerals-rich deposits pigmented with Fe-oxides and/or Fe-oxi-hydroxides; in addition, the same term is also used to designate natural Fe-based yellow and red pigments, also known as earthy pigments (Hradil *et al.*, 2003), widely used since the Palaeolithic times in burial practices, food preservation, decoration of the body, etc. However the most common application has been in the field of visual arts (Delamare & Guineau, 2000). Their wide occurrence in different geological environments, stability in all the organic and inorganic media and compatibility with all pigments and dyes, have been the guiding factors in deciding their popularity as the most common material in wall decorations and paintings (Helwig, 2007).

Although there is a general lack of consensus on the terminological meaning of ochre, it will be used here with the following connotation: clay minerals rich of Fe-based oxides having colouring power, generally in association with non-colouring mineral phases whose composition depends on the host and mother rocks, extent of alteration, eventual transport and depositional mechanisms.

Rajasthan State (NW India) is the leading producer of ochre in India (Mineral Directory of Rajasthan, 2008) where red and yellow deposits are reported from almost all the districts. In this paper the characteristics of red ochre collected from mines located in Chittourgarh district in the south-eastern part of the State will be discussed.

The research was aimed at characterizing the ochre deposits by correlating the mineralogical and chemical composition with the geological environment in order to infer the source and to identify possible markers useful for archaeometric purposes. Therefore, the present study represents a first step that would lead to implementation in archaeological and historical contexts as the characterization of the raw materials can be related with artworks for tracing the provenance (Popelka-Filcoff *et al.*, 2008; Grygar *et al.*, 2003). The other scientific significance of the study is that it provides mineralogical and geochemical data concerning Fe-based materials (Cavallo & Zorzin, 2008); micro-structural characteristics have provided useful information on the relationship between clay minerals and hematite (Hradil *et al.*, 2003). This basic information already is useful for proper interpretation of archaeologically significant ochre as the presence of mineral

phases such as calcite and dolomite could be interpreted as voluntary addition in the form of extenders wherever they are regarded as impurities inherited from the parent rock. Finally, this topic is quite new in India as no previous studies are available except those in the field of economic geology (Shekhawat & Sharma, 2009).

2. GEOLOGICAL SETTING

Precambrian rocks in NW India occur as a NE-SW trending, >750 km long tract beginning from south of Delhi in the north, to northern Gujarat in south. This terrain, also known as Aravalli Mountain Region (AMR) exposes two Proterozoic metasedimentary sequences: Aravalli (Paleoproterozoic) and Delhi (Mesoproterozoic) fold belts, deposited over an Archean basement popularly known as the Banded Gneiss Complex BGC (BGC: Heron, 1953; Fig. 1). A number of white mica and sericite rich deposits (<1 m to >10 m thick) occur in a linear array all along the Archean – Proterozoic contact around Udaipur city. These have been described as 'paleosol' or 'fossil soil' which show a gradational contact with the basement granite-gneisses (BGC) and a sharp one with the overlying metasediments of Aravalli Supergroup, characteristic of preserved in-situ soil profiles (Sreenivas *et al.*, 2001; Pandit *et al.*, 2008; de Wall *et al.*, 2012). Precambrian geological history of this region is marked with multiple phases of deformation and metamorphism, and the present day outcrop pattern is a result of the processes which have controlled the weathering conditions. The basement rocks are directly juxtaposed to the Meso-Neoproterozoic Vindhyan Supergroup along the Great Boundary Fault. In contrast to the other sequences, the Vindhyan rocks (sand – carbonate – shale) are undeformed and seen as horizontal to subhorizontal exposures in an East – West trending sickle-shaped basin running across central India. In the southern part of AMR, the Precambrian rocks are directly covered by Late Cretaceous – Early Paleogene Deccan Flood Basalts and Quaternary alluvium. The sampled sites for the present study are located in Chittourgarh district forming the south-central part of the AMR (Fig. 1).

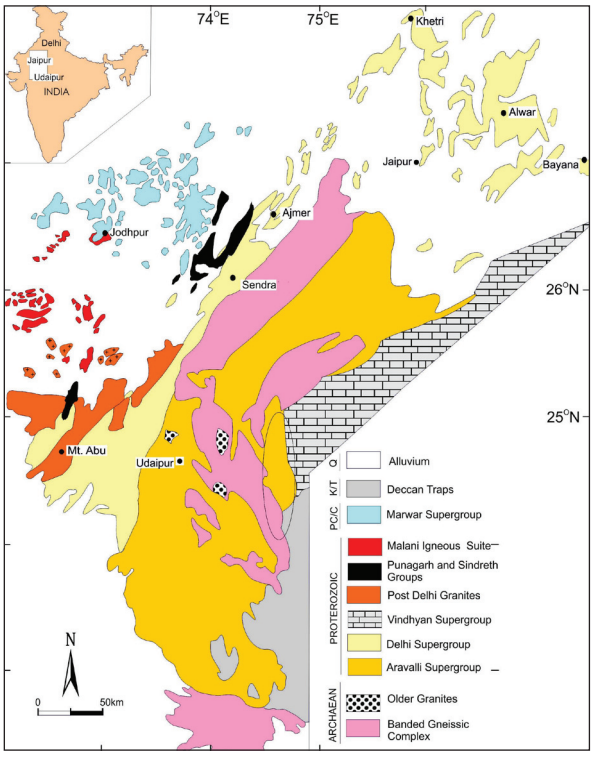

Fig. 1 – Schematic geological map of Rajasthan with indication (black ellipse) of the studied area. Map modified from van Lente *et al.*, 2009.

3. MATERIALS AND METHODS

Field visits were conducted at the active and abandoned mining pits for documenting geological observations and for collecting hand samples from the working faces or any other suitable surface. The description and location of the collected samples are reported in table 1.

Generally the samples are homogeneous in colour and textural characteristics. Polished thin sections of standard thickness (~30 µm) were prepared for examination in transmitted and incident lights using a Zeiss polarizing microscope. Selected areas of the thin sections were examined using a Scanning Electron Microscope coupled with an Energy Dispersive Spectrometer (SEM/EDS) in order to obtain the chemical elemental composition and for the mapping. A Jeol JSM-5910LV Scanning Electron Microscope was used, operating at the following conditions: 20 kV, LV mode (Pressure = 15 Pa), working distance 9 mm, spot size 37. The mineralogical composition was determined by means of X-Ray Diffraction (XRD) on randomly oriented powders of appropriate size (<150 mesh) using a Philips X' Pert Pro type PW

Samples	*Description*	*Location*
CH-02	Massive clay-rich Fe-oxides exhibiting small nodules ∅ = 3-5 mm	N 24°47′00″ E 74°35′00″
CH-03a	Massive and homogeneous clay-rich Fe-oxides exhibiting white variegations	N 24°47′00″ E 74°38′06″
CH-09a	Massive and homogeneous clay-rich Fe-oxides	N 24°52′18″ E 74°35′22″
CH-11b	Massive clay-rich Fe-oxides exhibiting off-white areas	N 24°47′06″ E 74°34′52″
CH-13b	Massive bauxite associated with minor clay-rich Fe-oxides	N 24°48′40″ E 74°35′04″
CH-15	Massive clay-rich Fe-oxides with off-white areas	N 24°49′02″ E 74°35′18″
CH-16	Centimetre massive Fe-oxides nodules intercalated with clay-rich Fe-oxides	N 24°24′06″ E 74°45′14″
CH-17	Massive and homogeneous clay-rich Fe-oxides; small nodules are visible	N 24°38′59″ E 74°31′40″

Tab. 1 – List of the collected samples, description and location.

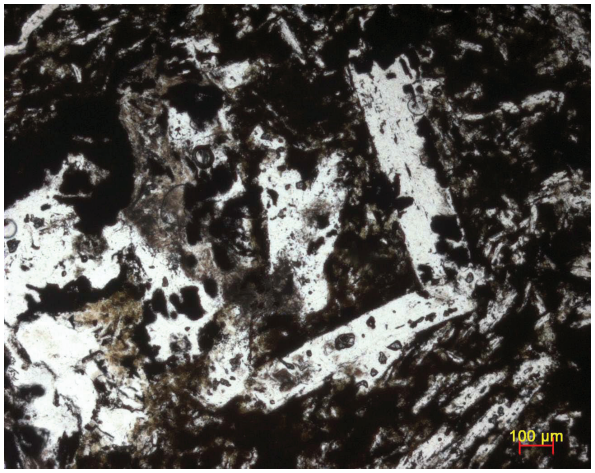

Fig. 2:1 – Sample CH15 (PPL). Plagioclase-like relics (pseudomorphs of clay minerals after plagioclase) in an isotropic ground mass (texture indicating basaltic source rock).

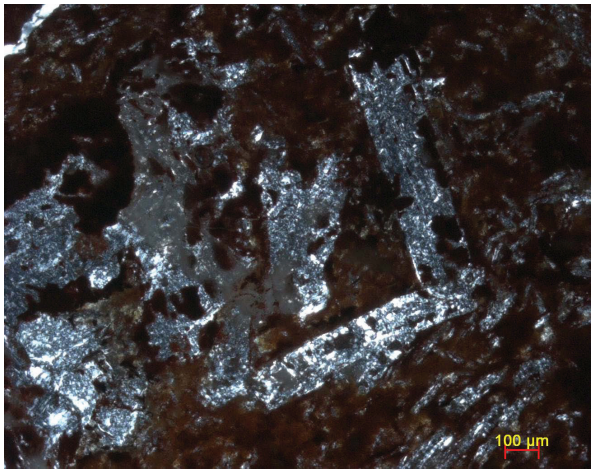

Fig. 2:2 – As figure 4:1, under XPOL.

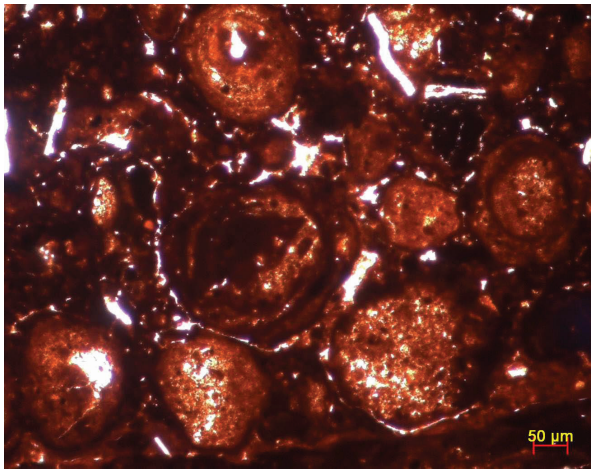

Fig. 2:3 – Sample CH02 exhibiting iron-rich glaebules cemented with secondary calcite (PPL).

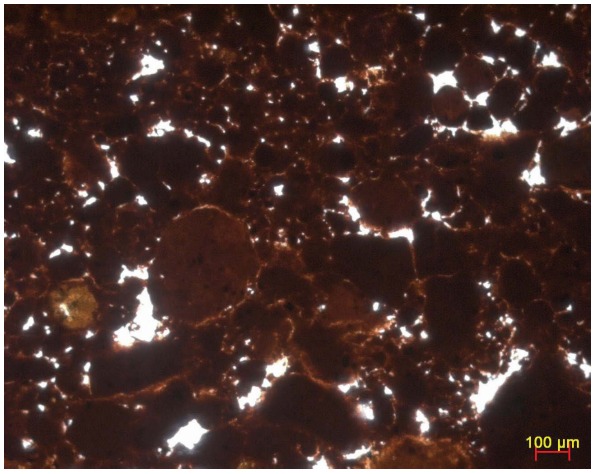

Fig. 2:4 – Sample CH17 exhibiting iron-rich glaebules cemented with secondary calcite (PPL).

Samples	*Description*
CH-02	Iron-rich based matrix and isotropic minerals having plagioclase shape. Sericite coming from the alteration of feldspars fills cavity and fissures. Presence of iron-rich ooids-like morphologies (glaebules) ∅~200-300 µm. Feldspars relics still visible.
CH-03a	Iron-rich based matrix and isotropic minerals having plagioclase shape.
CH-09a	Iron-rich based matrix and isotropic minerals having plagioclase shape.
CH-11b	Iron rich based matrix with secondary calcite veins.
CH-13b	Iron-rich based matrix associated with fine clay minerals with large crystals of calcite.
CH-15	Iron-rich based matrix associated with sericite and plagioclase shaped minerals. The basaltic texture of the mother rock is very well preserved.
CH-16	Iron-rich based matrix associated with traces of quartz, altered plagioclases and clay minerals.
CH-17	Iron-rich based matrix exhibiting iron-rich ooids-like morphologies (glaebules) ∅ ~100-200 µm; fractures are filled with secondary calcite. Rounded quartz grains are still preserved.

Tab. 2 – Characteristics of the collected samples under PLM.

3040/60; X-ray tube with Cu anti-cathode (40 kV, 20 mA). Working conditions: speed 1º 2θ/min, range 2°-65° 2θ.

XRF analysis of the major elements was performed at Wadia Institute of Himalayan Geology (India) on pressed pellets using Siemens SRS 3000 X-Ray Fluorescence Sequential Spectrometer. LOI (Loss on Ignition) contents were calculated as loss in weight after heating at 1000 °C and the elimination of hydration water at 110 °C.

4. RESULTS

4.1. Polarised Light Microscopy (PLM)

The characteristics of the studied samples under optical microscope are reported in table 2.

All the samples exhibit a reddish-brown isotropic groundmass and, in most cases, relics of plagioclase-like minerals (Fig. 2:1-2) where small and fibrous minerals are clearly visible (clay minerals); in other cases (samples CH02, CH17) rounded morphologies similar to ooids were detected. In particular, sample CH02 displays iron-rich glaebules with and without concentric fabric (Fig. 2:3); iron-rich glaebules in the sample CH17 do not show any concentric fabric (Fig. 2:4). The lack of concentric fabric corresponds to the undifferentiated fabric proposed by Brewer and Sleeman (1964). The iron-rich glaebules are the consequence of ferruginous segregation typical of tropical and sub-tropical regions (Singh & Gilkes, 1996).

Opaque minerals of irregular shape are quite abundant in all the samples. Deep red hexagonal crystals of hematite are clearly recognizable as very thin plates.

Samples CH11b, CH13b and CH17 show the presence of calcite as the cementing material derived from dissolution and re-precipitation processes; rhombohedral crystals showing multiple twinning are seen well preserved in the sample CH13b.

Detrital fraction is represented by small amounts of quartz (samples CH11b, CH17).

4.2. Scanning Electron Microscopy coupled with Energy-Dispersive X-Ray Spectrometer (SEM/EDS)

Selected areas of a few samples were examined under PLM and considered for in-depth studies (samples CH02, 15, 16, 17) focusing mainly on the materials exhibiting an ooid-like morphologies corresponding to glaebules (CH02 and CH17).

Sample CH02 exhibits different types of rounded morphologies ∅ ~100 µm where Si, Al, Fe and Ti have variable concentration. These microstructures are clearly distinguishable from the surrounding matrix and can be grouped as follows according to the relative amount displayed in the X-ray mapping (Fig. 3:1-5; Fig. 4:1-5):

- Type A: Fe-rich cores ∅ ~70 µm surrounded by a thin Al-rich rim where Fe and Al are individual

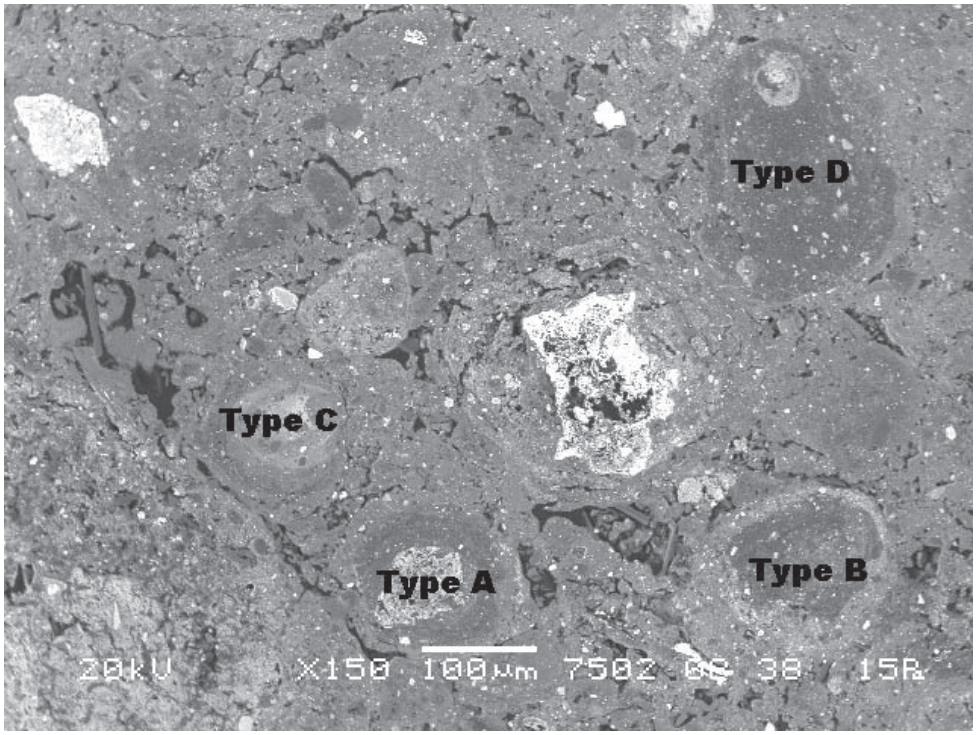

Fig. 3:1 – BSE image of an area corresponding to sample CH02. The four types A-D of glaebules are presented.

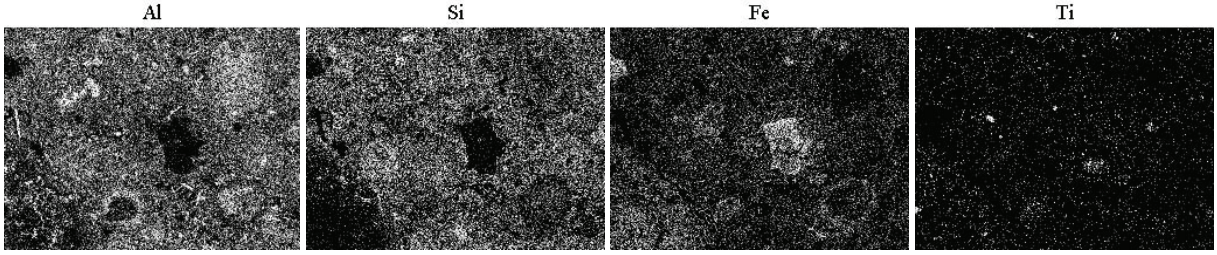

Fig. 3:2 – Al X-ray mapping. **Fig. 3:3** – Si X-ray mapping. **Fig. 3:4** – Fe X-ray mapping. **Fig. 3:5** – Ti X-ray mapping.

grains (Fe and Al oxides) and Al is also related with Si. It is not possible to exclude a correlation between Fe-Al-Si as well.

- Type B: Al-rich cores ∅ ~100 µm, occasionally ∅ ~250 µm, surrounded by a thin Fe-rich rim where Al is both related with individual grains (Al-oxides) and Si. Fe is in the form of individual grains (Fe-oxides) and a correlation between Fe-Al-Si cannot be excluded as well due to Al replacement.
- Type C: Al-Si rich cores ∅ ~85 µm where Al is both related to Al-oxides individual grains and to Si surrounded by a Al-Si rim.
- Type D: Al-rich sub-rounded particles ∅ ~130-210 µm where Al is both related to Al-oxides individual grains and to Si.

Al and Fe-based individual grains are normally very small having size ranging between 5-10 µm; Fe-based individual grains exhibiting irregular morphology (75 µm large and 115 µm long) are quite rare. Ti is spread within the Si-Al matrix.

Sample CH17 exhibits glaebules (∅ ~200-400 µm) without internal micro-structure composed of Si, Al and Fe and cemented with calcite (Fig. 5:1-6). A detailed analysis of one of them confirms the association between Al and Si (clay minerals of the kaolin group). Fe is spread and individual Fe, Ti and Fe-Ti-containing grains are clearly recognizable. It is not possible to exclude Al replacement by Fe in the clay minerals structure as for the previous groups.

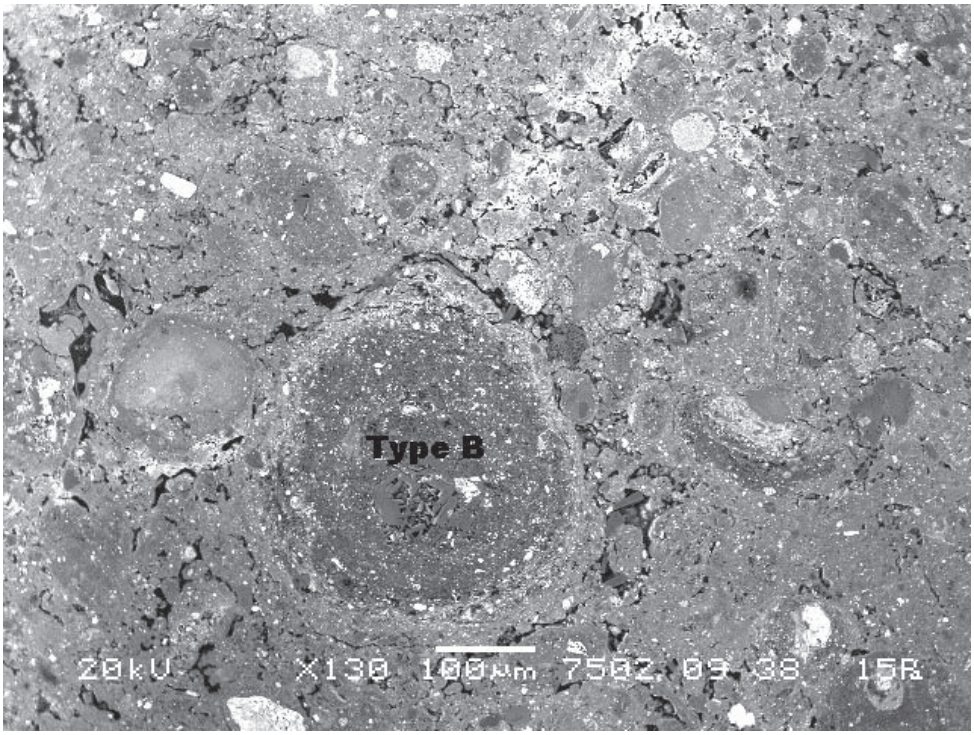

Fig. 4:1 – BSE image of an area corresponding to sample. CH02. Glaebule type B is displayed.

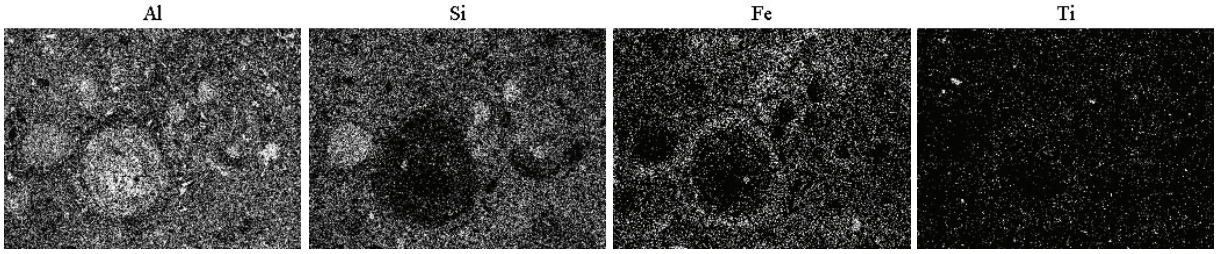

Fig. 4:2 – Al X-ray mapping. **Fig. 4:3** – Si X-ray mapping. **Fig. 4:4** – Fe X-ray mapping. **Fig. 4:5** – Ti X-ray mapping.

Many samples analysed under PLM (Cavallo & Pandit, 2008) exhibit tabular pseudo-crystals distributed randomly within the ferruginous matrix looking like plagioclases as reported in figure 2:1 and table 1. Al and Si elemental X-ray maps (sample CH15) suggest they correspond to clay minerals of the kaolin group (Fig. 6:1-6); minor quantities of Fe and Ti are associated as well. Crystals of hematite (maximum grain size ~200 µm) were also detected.

4.3. X-Ray Diffraction (XRD)

Mineral phases of the collected samples are reported in table 3.

All the samples contain kaolinite, hematite and anatase. Kaolinite exhibits different degrees of structural order-disorder (Brindley, 1984).

The sample CH13b (Fig 7) shows the basal reflections 001 and 002 at 12.4° and 24.9° 2θ sharp and intense; the reflections in the range 20°-33° 2θ are well defined; finally, in the range 35°-40° 2θ the reflections corresponding to the indices 131, 201 and basal 003, form two groups of triplets. All these reflections indicate an ordered structure.

In all the remaining samples the disorder increases (Fig. 8): the basal reflections 001 and 002

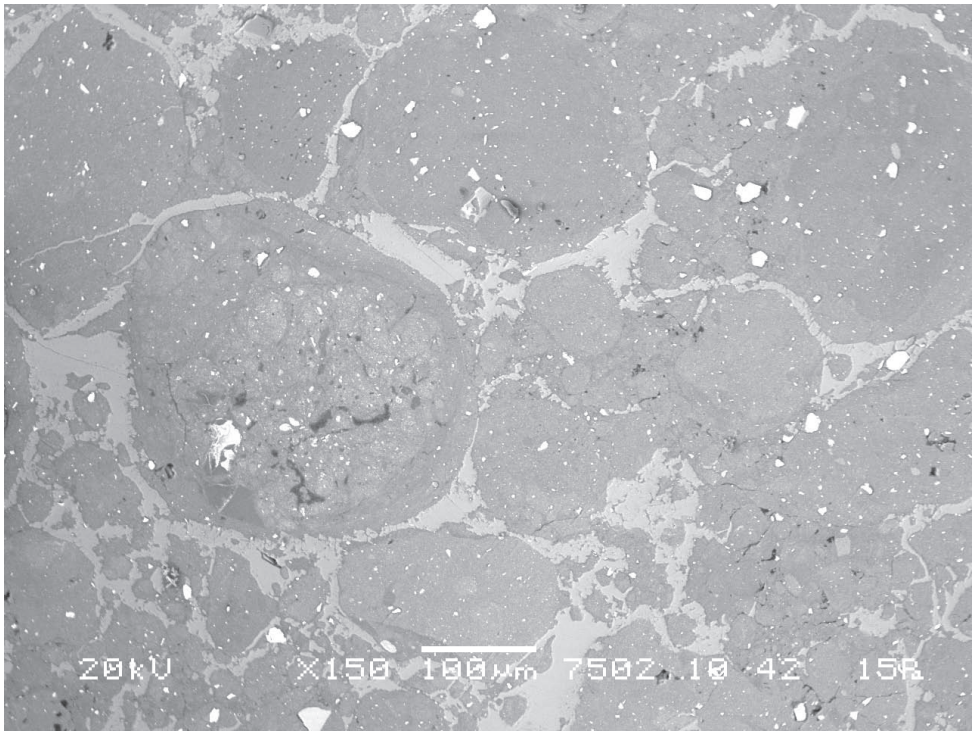

Fig. 5:1 – BSE picture of an area corresponding to sample n. CH17: glaebules type B showing shrinkage cracks and incorporation of detrital grains.

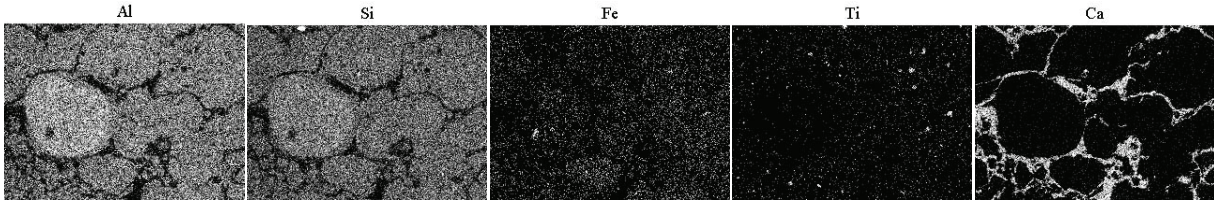

Fig. 5:2 – Al X-ray mapping.

Fig. 5:3 – Si X-ray mapping.

Fig. 5:4 – Fe X-ray mapping.

Fig. 5:5 – Ti X-ray mapping.

Fig. 5:6 – Ca X-ray mapping.

are less sharp; the reflections in the range 20°-33° 2θ are blurred (the reflection at about 20.4° 2θ is missing) and the two triplets become two doublets.

According to the characteristics of the reflections, kaolinite structure can be classified in two groups:

- Type I: ordered kaolinite (samples CH11b, CH13b, CH17);
- Type II: disordered kaolinite (samples CH02, CH3a, CH9a, CH15, CH16).

For all the samples the reflections due to hematite are broad indicating poor-crystalline mineral; the same considerations are valid for anatase. In the samples CH09a (probably), CH13b and CH16 hematite is associated with small quantities of goethite.

Gibbsite [$Al(OH)_3$] shows the sharp reflections 002 (100 %) and 110 (40 %) in all the samples where it was detected (CH02, CH13b).

Calcite [$CaCO_3$] was detected in the samples CH11b, CH13b, CH17. Quartz [SiO_2] in the samples CH11b, CH16, 17 and Zircon [$Zr(SiO_4)$] in the sample CH16 were finally detected.

4.4. X-Ray Fluorescence (XRF)

The results of XRF-analyses of the collected samples are presented in table 4.

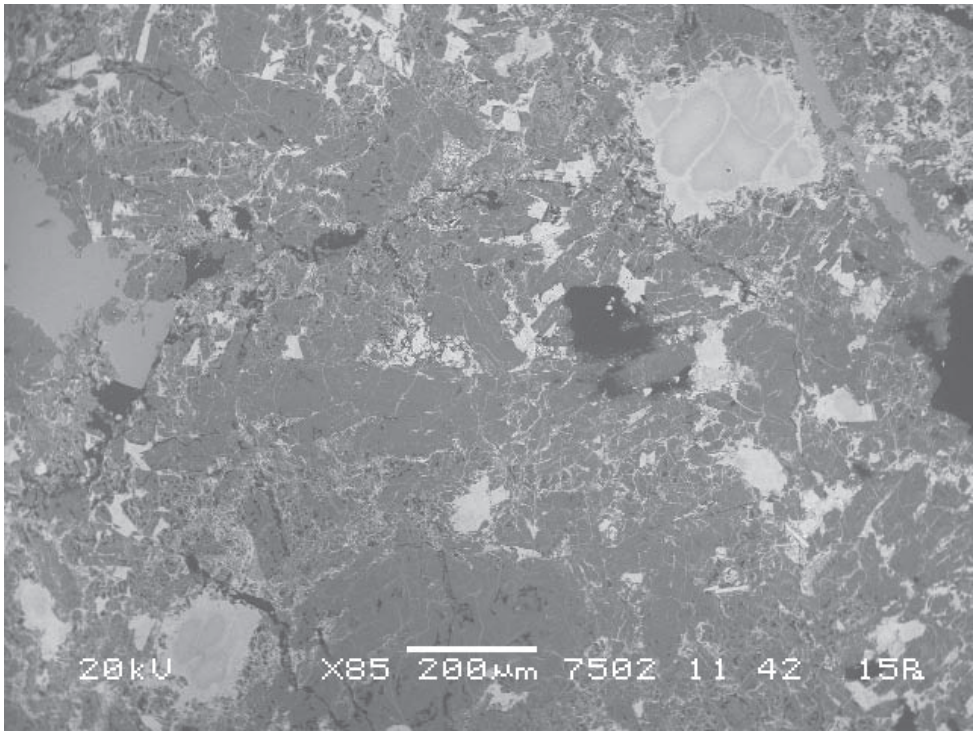

Fig. 6:1 – BSE image of an area corresponding to sample CH15. Crystals of hematite are high-reflective grains in the upper (right side) and lower part (left side) of the micrograph.

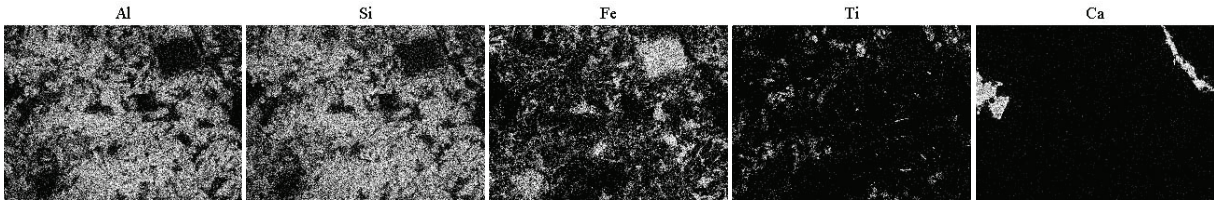

Fig. 6:2 – Al X-ray mapping.

Fig. 6:3 – Si X-ray mapping.

Fig. 6:5 – Ti X-ray mapping.

Fig. 6:4 – Fe X-ray mapping.

Fig. 6:6 – Ca X-ray mapping.

Samples	Minerals
CH-02	Hem, Gbs, Kln, Ant
CH-03a	Hem, Kln, Ant
CH-09a	Kln, Hem, Ant, Gt?
CH-11b	Qtz, Kln, Hem, Ant, Cal
CH-13b	Kln, Hem, Ant, Gt, Gbs, Cal
CH-15	Hem, Kln, Ant
CH-16	Qtz, Hem, Ant, Gt, Kln, Zrn,
CH-17	Kln, Hem, Cal, Ant, Qtz

Hem = hematite
Gbs = gibbsite
Kln = kaolinite
Ant = anatase
Gt = goethite
Qtz = quartz
Cal = calcite
Zrn = zircon

Tab. 3 – XRD of the samples with indication of the mineral phases.

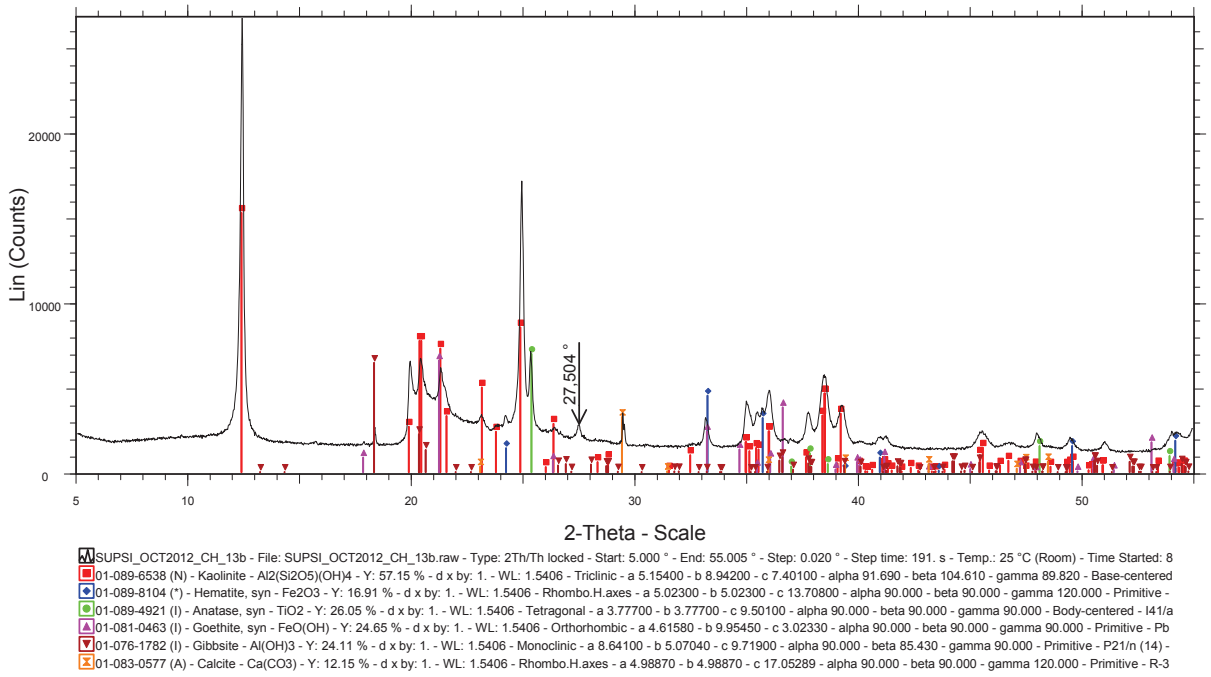

Fig. 7 – XRD of the sample CH13b displaying well-ordered kaolinite.

All samples have >10% LOI (except sample CH11b) underlining their heavily altered nature. Negligible alkali contents, further substantiate this interpretation as these are highly mobile in any crustal process. Both Al and Ti are extremely resistant and immobile during hydration and alteration processes. An inverse relationship between SiO_2 and TiO_2 also attests this proposition (Tab. 4:1).

TiO_2 values are unusually high and also correlate positively with Al_2O_3 (Tab. 4:2). The SiO_2 correlates positively with LOI, further confirming that the SiO_2 was the major component lost during alteration. High and variable Fe_2O_3 values suggest both an iron rich source rock as well as iron enrichment during alteration process; Fe_2O_3 enrichment is negatively correlated with SiO_2 (Tab. 4:3); SiO_2 is positively correlated with Al_2O_3 (Tab. 4:4) indicating both components related with kaolinite with the exception where quartz and gibbsite are present. Al_2O_3 values are negatively correlated with Fe_2O_3 (Tab. 4:5).

Lack of any systematic correlation between

Samples	SiO_2	Al_2O_3	CaO	MgO	Fe_2O_3	Na_2O	K_2O	TiO_2	P_2O_5	LOI
CH02	17.33	24.67	0.08	0.00	44.55	0.00	0.00	6.58	0.05	11.58
CH03a	25.23	21.38	0.13	0.00	35.52	0.00	0.00	4.62	0.23	11.24
CH09a	26.34	22.09	0.14	0.12	29.07	0.00	0.00	9.69	0.09	10.58
CH11b	33.02	16.60	1.16	0.00	35.35	0.00	0.14	3.19	0.04	8.16
CH13b	38.76	34.46	2.23	0.00	3.55	0.00	0.00	3.12	0.00	14.79
CH15	32.01	24.66	0.71	0.07	21.90	0.00	0.00	5.10	0.05	13.09
CH16	16.20	14.93	0.05	0.00	50.00	0.00	0.04	2.48	0.27	13.26
CH17	29.62	24.50	5.36	0.06	19.22	0.00	0.00	5.61	0.04	14.47

Tab. 4 – XRF analysis of the major elements (wt%).

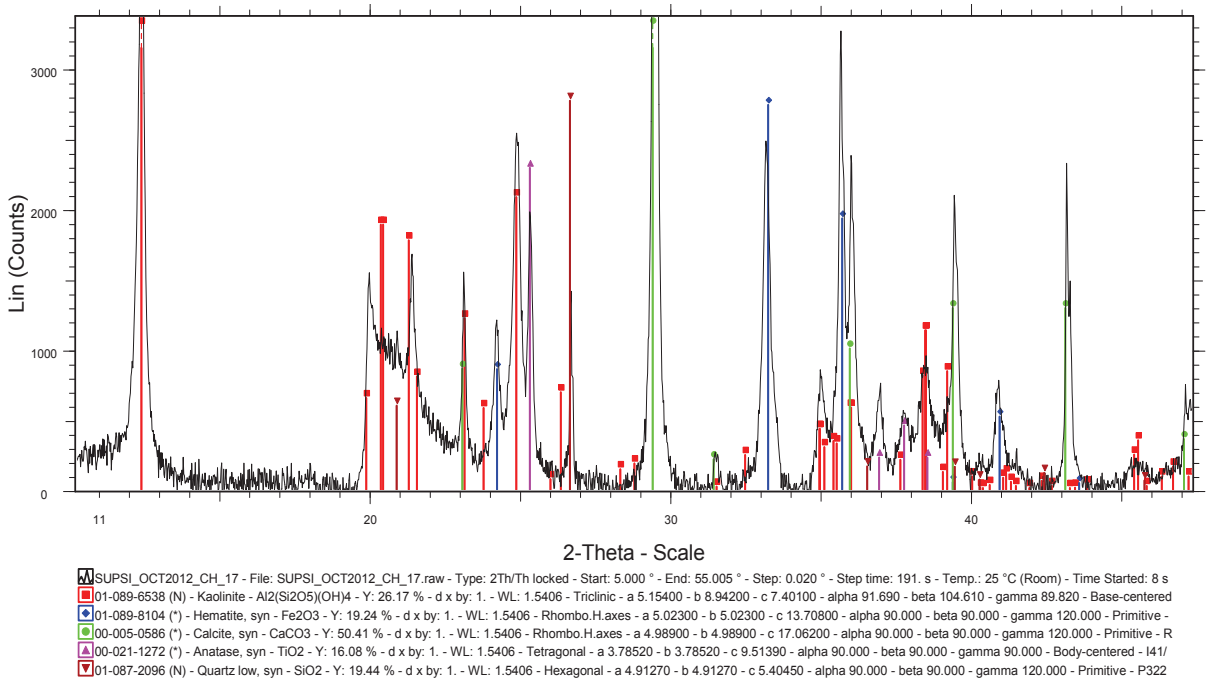

Fig. 8 – XRD of the sample CH17 displaying disordered kaolinite.

TiO_2 and Fe_2O_3 suggests secondary iron enrichment during alteration.

Overall geochemistry (low SiO_2, high Al_2O_3, TiO_2 and Fe_2O_3) indicate basic rocks (most likely, basalt) as the provenance for these iron rich clays.

5. DISCUSSION

The petrographic examination of the studied samples was aimed at establishing the mineralogical composition of the detrital fraction and of the cementing material and the microstructure.

The detrital fraction is limited to quartz grains just in a few samples (samples CH11b, CH16, CH17) indicating an advanced alteration process and/or a basic source. The advanced alteration process is related with Fe enrichment as also confirmed by the geochemistry (Fig. 9:3). Samples CH11b, CH13b, CH17 contain calcite which is related to dissolution processes of carbonate rocks and to later precipitation in the form of secondary calcite cement.

Most of the samples exhibit plagioclase-like ghosts; microanalysis allowed to infer their nature which is correlated with the presence of kaolinite, as confirmed by XRD. The microstructure is very similar to basaltic rocks suggesting basic rocks as possible source material; in addition, the geochemistry (low SiO_2 and high Al_2O_3, TiO_2 and Fe_2O_3 contents) confirms the observations under PLM.

The majority of the samples have a massive structure and samples CH02 and CH17 exhibit glaebules. SEM/EDS analysis allowed to identify, in the first sample, four sub-types of glaebules on the basis of Fe, Al and Si distribution. According to the analytical data, it seems that the formation of these morphologies do not follow a specific trend as, in the same micro-area, four different distributions were detected.

In all the samples, Fe and Si+Al corresponding respectively to hematite and kaolinite, are simultaneously present and well cemented leading to a high stability. Such an interaction between iron oxides and kaolinite has also been documented in some other studies (Wei *et al.*, 2012; Sengupta *et al.*, 2008).

In the analysed samples kaolinite is generally disordered as the blurred reflections in the range 20°-33° 2θ and the two doublets instead of

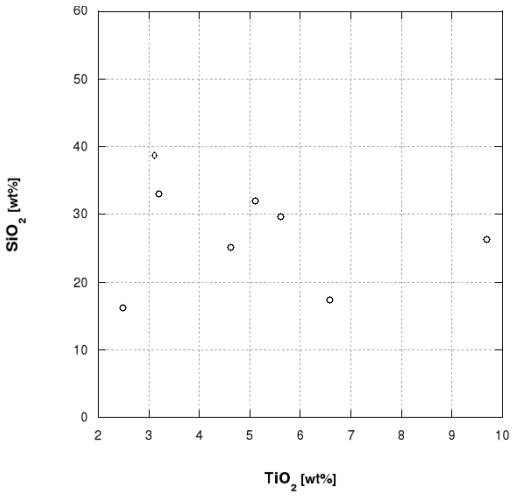

Fig. 9:1 – SiO_2-TiO_2 plot.

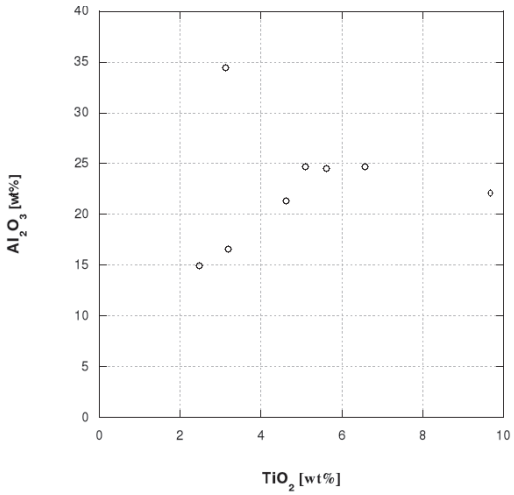

Fig. 9:2 – Al_2O_3-TiO_2 plot.

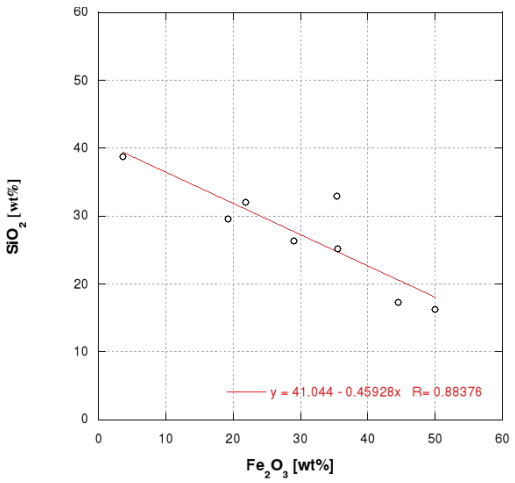

Fig. 9:3 – SiO_2-Fe_2O_3 plot.

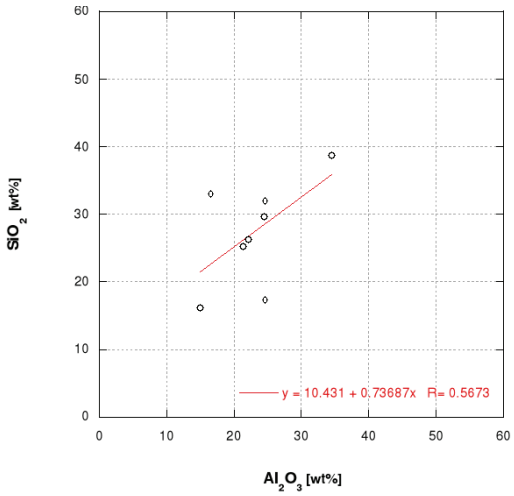

Fig. 9:4 – SiO_2-Al_2O_3 plot.

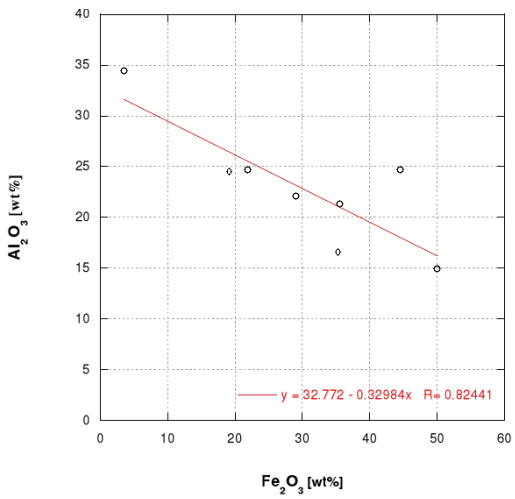

Fig. 9:5 – Al_2O_3-Fe_2O_3 plot.

the two triplets in the range 25°-40° 2θ clearly indicate. The disorder can be the consequence of an intense alteration and/or Al replacement by Fe in the kaolinite structure.

Hematite reflections are very broad indicating a poor-crystalline mineral phase.

The positive correlation between Al and Ti is not evident in all the samples even if a positive trend can be seen in a few samples indicating the progressive anatase enrichment with kaolinite progressive formation. The negative correlation between Al and Fe is more clear in almost all the samples, indicating a progressive hematite enrichment.

Finally mineralogical and geochemical data allow to infer basic rocks (most likely, basalt) as the provenance for these iron rich clays and related to a post Tertiary weathering and alteration of Deccan basalts.

6. CONCLUSION

The research carried out on kaolinitic hematite overlying the Precambrian formations of Chittourgarh area in Rajasthan State (NW India) allowed to differentiate the analysed materials on the basis of mineral composition, micromorphology, microstructure, kaolinite structure and geochemistry of the major elements.

The correlation with source rocks corresponding to Deccan basalts exposed in this region and volumetrically minor high silica ones can be associated with shale and sandstones belonging the Vindhyan Supergroup. It seems quite likely that the ochre represent partially preserved paleosols developed over the host rocks.

Our findings have shown that ochre chemistry and petrography can be interpreted in terms of host lithologies.

This research can be used to trace the provenance of iron-rich clays in historic and archaeological contexts aware that an in-depth study of the regional geology and geochemistry of minor and trace elements would be necessary.

Acknowledgements

We are thankful to the two reviewers for critical comments and very useful suggestions that have helped in improving the manuscript. The study is part of the project *Geology, Mineralogy and Geochemistry of ochre in Rajasthan (India)* partially supported by the Swiss Agency for Development and Cooperation SDC (grant no. P-0710-04).

Bibliography

BREWER R. & SLEEMAN J. R., 1964. Glaebules: their definition, classification and interpretation. *Journal of Soil Science*, **15** (1): 66-78.

BRINDLEY G. W., 1984. Order-disorder in clay mineral structure. *In*: G. W. BRINDLEY & G. BROWN (ed.), *Crystal Structure of Clay Minerals and their X-Ray Identification*. Mineralogical Society, Monography no. 5, London: 146-149.

CAVALLO G. & PANDIT M. K., 2008. Geology and petrography of ochers and white clay deposit in Rajasthan State, India. *In*: R. I. KOSTOV, B. GAYDARSKA & M. GUROVA (ed.), *Geoarchaeology and Archaeomineralogy*: 147-152.

CAVALLO G. & ZORZIN R., 2008. Preliminary data on the yellow ochers at the mine of Via Tirapelle in Verona. Italy. *X-Ray Spectrometry,* **37**: 395-398.

DELAMARE F. & GUINEAU B, 2000. *Colors. The story of pigments and dyes.* Harry N. Abrams Inc., New York.

DE WALL H., PANDIT M., K., CHAUHAN N. K, 2012. Paleosol at the Archean - Proterozoic contact in Udaipur. *Precambrian Research*, **216-219**: 120–131.

GRYGAR T., HRADILOVA J., HRADIL D., BEZDICKA P. & BAKARDJIEVA S., 2003. Analysis of earthy pigments in grounds of Baroque paintings. *Analytical* and *Bioanalytical Chemistry,* **375**: 1154-1160.

HELWIG K., 2007. Iron Oxide Pigments. Natural and Synthetic. *In*: B. H. BERRIE (ed.), *Artist's Pigments,* Washington: National Gallery of Art, **4**: 39-109.

HERON A. M., 1953. Geology of Central Rajputana. *Memoir Geological Society of India*, **79**: 339 p.

HRADIL D., GRYGAR T., HRADILOVA J. & BEZDICKA P., 2003. Clay and iron oxide pigments in the history of painting. *Applied Clay Science*, **22**: 23-236.

MINERAL DIRECTORY OF RAJASTHAN, 2008. *Mineral resources in Rajasthan*. Department of Mines and Geology, published by Government of Rajasthan.

PANDIT M. K., DE WALL H. & CHAUHAN N. K., 2008. Paleosol at the Archean – Proterozoic contact revisited: evidence for oxidizing conditions during palaeoweathering? *Journal of Earth System Sciences*, **117**: 201-209.

POPELKA-FILCOFF R. S., MIKSA E. J., ROBERTSON J. D., GLASCOCK M. D. & WALLACE H., 2008. Elemental analysis and characterization of ochre sources from Southern Arizona. *Journal of Archaeological Science*, **35**: 752-762.

SENGUPTA P., SAIKIA P. C. & BORTHAKUR P. G., 2008. SEM-EDX characterization of an iron-rich kaolinite clay. *Journal of Scientific & Industrial research*, **67**: 812-818.

SINGH B. & GILKES R. J., 1996. Nature and properties of iron-rich glaebules and mottles from southwest Australian soils. *Geoderma*, **71**: 95-120.

SHEKHAWAT M. S. & SHARMA V., 2009. Mineralogical characteristics and mineral economics of kaolinite deposit of Sawa area, Chiittaurgarh, Rajasthan. *Journal Geological Society of India*, **74**: 27-34.

SREENIVAS B., ROY A. B. & SRINIVASAN R., 2001. Geochemistry of sericite deposits at the base of the Paleoproterozoic Aravalli Supergroup, Rajasthan, India: evidence for metamorphosed and metasomatised Precambrian Paleosol. *Proceedings of the Indian Academy of Sciences, Earth and Planetary Sciences*, **110** (1): 39-61.

VAN LENTE B., ASHWAL L. D., PANDIT M. K., BOWRING S. & TORSVIK T. H., 2009. Neoproterozoic hydrothermally altered basaltic rocks from Rajasthan, northwest India: Implications for late Precambriam tectonic evolution of the Aravalli Craton. *Precambrian Research*, **170**: 202-222.

WEI S., TAN W., ZHAO W., FAN LIU Y. Y. & KOOPAL L. K., 2012. Microstructure, interaction mechanisms and stability of binary systems containing goethite and kaolinite. *Soil Science Society of America Journal*, **76** (2): 389-398.

Authors address:

Giovanni CAVALLO
Department of Earth and Environmental Sciences
University of Pavia (Italy)
giovanni.cavallo01@ateneopv.it
and
Institute of Materials and Constructions
DACD-SUPSI
Canobbio (Switzerland)
giovanni.cavallo@supsi.ch

Manoj K. PANDIT
Department of Geology
University of Rajasthan
Jaipur 302003 (India)
manoj.pandit@gmail.com